HHS Public Access

Author manuscript

Int J Cardiol. Author manuscript; available in PMC 2016 August 01.

Published in final edited form as:

Int J Cardiol. 2015 August 1; 192: 61–69. doi:10.1016/j.ijcard.2015.05.020.

Exosomes/microvesicles from induced pluripotent stem cells deliver cardioprotective miRNAs and prevent cardiomyocyte apoptosis in the ischemic myocardium

Yingjie Wang, MD, Ph.D[1,*], **Lan Zhang, MD, PhD**[2,*], **Yongjun Li, MD, Ph.D**[3,6,*], **Lijuan Chen, MD, PhD**[3,*], **Xiaolong Wang, MD**[1], **Wei Guo, MD**[1], **Xue Zhang, MD**[2,6], **Gangjian Qin, MD**[4], **Sheng-hu He, MD**[5], **Arthur Zimmerman, MS**[6], **Yutao Liu, Ph.D**[6], **Il-man Kim, Ph.D**[6], **Neal L. Weintraub, MD**[6], and **Yaoliang Tang, MD, PhD**[6]

[1]Internal Medicine of Traditional Chinese Medicine, Shuguang Hospital of Shanghai University of Traditional Chinese Medicine, Shanghai, 201203, China

[2]Department of Vascular Surgery, Renji Hospital, School of Medicine, Shanghai Jiaotong University, Shanghai, 200127, China

[3]Department of Cardiology, Zhongda Hospital, Medical School of Southeast University, Nanjing, China

[4]Feinberg Cardiovascular Research Institute, Northwestern University Feinberg School of Medicine, Chicago, IL 60611

[5]Subei People's Hospital of Jiangsu Province, Yangzhou, Jiangsu, 225001, China

[6]Medical College of Georgia, Georgia Regents University, 1459 Laney Walker Blvd, Augusta, GA 30912

Abstract

Background/Objectives—Induced pluripotent stem cells (iPS) exhibit enhanced survival and proliferation in ischemic tissues. However, the therapeutic application of iPS cells is limited by their tumorigenic potential. We hypothesized that iPS cells can transmit cytoprotective signals to cardiomyocytes via exosomes/microvesicles.

Methods—Exosomes/microvesicles secreted from mouse cardiac fibroblast (CF)-derived iPS cells (iPS-exo) were purified from conditioned medium and confirmed by electron micrograph,

Correspondence to: Yaoliang Tang, MD, PhD, FAHA, Associate Professor of Cardiovascular Medicine, Vascular Biology Center, Medical College of Georgia/Georgia Regents University, 1459 Laney Walker Blvd, Augusta, GA 30912. Telephone: (706)-721-8467, yaotang@gru.edu or Xiaolong Wang, wxlqy0214@163.com.

*These authors contributed equally to this publication

Conflicts of interest statement

The authors confirm that there are no conflicts of interest.

size distribution and zeta potential by particle tracking analyzer and protein expression of the exosome markers CD63 and Tsg101.

Results—We observed that exosomes are at low zeta potential, and easily aggregate. Temperature affects zeta potential (−14~−15mV at 23°C vs −24mV at 37°C). The uptake of iPS-exo protects H9C2 cells against H_2O_2-induced oxidative stress by inhibiting caspase 3/7 activation ($P<0.05$, n=6). Importantly, iPS-exo treatment can protect against myocardial ischemia/reperfusion (MIR) injury via intramyocardially injection into mouse ischemic myocardium before reperfusion. Furthermore, iPS-exo deliver cardioprotective miRNAs, including nanog-regulated miR-21 and HIF-1α-regulated miR-210, to H9C2 cardiomyocytes in vitro.

Conclusions—exosomes/microvesicles secreted by iPS cells are very effective at transmitting cytoprotective signals to cardiomyocytes in the setting of MIR. iPS-exo thus represent novel biological nanoparticles that offer the benefits of iPS cell therapy without the risk of tumorigenicity and can potentially serve as an " off-the-shelf" therapy to rescue ischemic cardiomyocytes in conditions such as MIR.

Keywords

Induced pluripotent stem cells; exosomes/microvesicles; Myocardial ischemia/reperfusion; Apoptosis

Background/Objectives

Acute myocardial ischemia/reperfusion (MIR) leads to cardiomyocyte loss by necrosis, and apoptosis. Because endogenous cardiomyocyte renewal is limited, MIR frequently leads to left ventricular remodeling and progressive heart failure[1]. Transplantation of stem cells into the heart can foster heart regeneration and improve systolic function in animals and humans following MIR[2]. Induced pluripotent stem cells (iPS cells), derived from somatic cells reprogrammed by four stem cell transcription factors, Oct4, Sox2, Klf4, and c-Myc, are a promising source of stem cell-based therapy for heart regeneration[3], however, the iPS derivates (iPSD) can form tumors, and tumorigenicity of iPSD is a major obstacle for therapeutic application of iPS [4].

Transplanted iPS cells exhibit enhanced survival in ischemic tissues, and also produce paracrine effects that promote survival of native cells within ischemic tissues. Lee et al [5] reported that iPS cells elicit antioxidant, anti-inflammatory, and anti-apoptotic effects in acute kidney ischemia-reperfusion injury. However, the mechanisms whereby iPS cells transmit pro-survival signals are largely unknown. Stem cells can secrete exosomes/microvesicles (30–150 nm), which shuttle microRNAs (miRNA) between cells, and play an important role in miRNA communication between donor stem cells and recipient tissues [6]. However, little is known about the functional effects of exosomes/microvesicles secreted by iPS cells. Since iPS cells exhibit a pronounced capacity to survive in ischemic myocardium, in this study, we evaluated whether exosomes/microvesicles secreted by iPS (iPS-exo) would be highly effective at promoting cardiomyocyte survival in vitro and in vivo in a mouse model of acute MIR.

Methods

Cell culture and Exosome purification

Murine cardiac fibroblasts (CF) and CF-derived iPS were established and maintained as we described previously[7]. Briefly, cardiac fibroblasts were infected with 1:1:1:1 mix of lentiviral vectors expressing Oct4, Sox2, Klf4, and c-myc with 8 μg/mL polybrene (Sigma-Aldrich). At 72 h after infection, the medium was replaced with mouse ES cell culture medium (DMEM high glucose with 15% FBS, 0.10 mM nonessential amino acids [Life Technologies], 100 U/mL penicillin G, 100 μg/ml streptomycin, 2 mM Glutamax [Life Technologies], and 0.1 mM β-mercaptoethanol, and 1000 units/ml Leukemia Inhibitory Factor [LIF] ESGRO® [Millipore]). The iPS cells colonies were identified, and verified by their pluripotency and tumorigenic potential as we described previously[7]. Mouse iPS cell colonies were dissociated with HyClone® HyQTase™ (Thermo) and passage into 0.1% gelatin coated dish containing mouse ES cell culture Medium. The media was replaced every other day and culture as normal. We use iPS in passages 10 to 15 for experiments.

Exosomes/microvesicles secreted by cardiac fibroblasts (CF-exo) and iPS cells (iPS-exo) were purified from conditioned medium as described previously [8, 9]. Briefly, 10 ml culture medium (CM) with 10% exosome-depleted FBS was added to CF or iPS cell cultures in 10 cm dishes. After 48hrs, medium was centrifuged at 1000 r.p.m. for 10min and the supernatant passed through 0.22μm filters to remove cell debris.

Exosomes/microvesicles were precipitated with 1/3 volume of polyethylene glycol (PEG) buffer (33.4% PEG 4000, 50 mM HEPES (pH 7.4), 1 M NaCl) overnight at 4°C followed by centrifugation at 3,000 rpm for 30 min. Exosomes/microvesicles were then resuspended in PBS, with the volume indexed to the number of cells from which the exosomes/microvesicles were derived (50μl PBS/5×10^6 cells), and stored at −80°C. We measured the exosome particle size and concentration using nanoparticle tracking analysis (NTA) with ZetaView PMX 110 (Particle Metrix, Meerbusch, Germany) and corresponding software ZetaView 8.02.28. Isolated exosome samples were appropriately diluted using 1X PBS buffer (Life Technologies, Carlsbad, CA, USA) to measure the particle size and concentration. NTA measurement was recorded and analyzed at 11 positions. The ZetaView system was calibrated using 100 nm polystyrene particles. Temperature was maintained around 23°C and 37°C. Zeta potential was measured using 0.05X PBS instead of 1X PBS to adjust conductivity to be around 500 uS/cm.

Electron microscopy

For transmission electron microscopy (TEM), 3μl of PBS containing exosomes/microvesicles was placed on formvar carbon-coated 200-mesh copper electron microscopy grids, incubated for 5min at room temperature (RT), and subjected to standard uranyl acetate staining[9, 10]. The grid was washed with three exchanges of PBS and allowed to semi-dry at room temperature before being imaged by TEM (JEOL JEM-1230 TEM, Peabody, MA). Micrographs were used to quantify the diameter of exosomes/microvesicles.

Western blotting

Exosomes/microvesicles were assessed for their protein content using BCA Protein Assay Kit (Pierce, Rockford, IL), and proteins were resolved on a 10% sodium dodecyl sulfate bis-tris gel and transferred to an Immobilon® FL PVDF membrane (Millipore, Billerica, MA). Membranes were blocked with Odyssey blocking buffer (LICOR Biosciences, Lincoln, NE) and probed with rabbit anti-CD63 (1:250, Santa Cruz Biotechnology, Inc., Santa Cruz, CA), mouse anti-TSG101 (1:250, Thermo Pierce), rabbit anti-HIF-1α (1:250, Santa Cruz Biotechnology Inc.), rabbit anti-mouse Nanog (1:1000, Cell signaling Technology, Beverly, MA), mouse anti-GAPDH (1:4000, Millipore), and then IRDye 680 goat anti-rabbit IgG at 1:5,000 (LICOR Biosciences) or IRDye 800 goat anti-mouse IgG at 1:5,000 (LICOR Biosciences). Probed blots were scanned using an Odyssey infrared imager(LI-COR Biosciences, Lincoln, Nebraska). Proteins from heart tissues were electroblotted onto membranes, and incubated with the Rabbit anti-active Caspase 3 (1:500, Sigma) overnight at 4°C. Then, they were incubated for 1 h at room temperature with Amersham ECL peroxidase-lined secondary antibodies: sheep anti-mouse IgG (1:10,000, GE Healthcare) or donkey anti-rabbit IgG (1:10,000, GE Healthcare). Western blot immunoreactivity was detected using a Super Signal West Femto Maximum Sensitivity Substrate Kit (Thermo) in C-DiGit Blot Scanner (LI-COR Biosciences, Lincoln, Nebraska).

Isolation and quantification of microRNAs

Total RNA from CF-exo or iPS-exo was extracted by RNAzol RT (Molecular Research Center, Inc. Cincinnati, OH) following the manufacturer's instructions. Isolated RNAs were polyadenylated using Ncode miRNA first-strand cDNA synthesis kits (Invitrogen). The cDNA synthesized was used to perform quantitative PCR on an Mx3000P Real-Time PCR System (Agilent Technologies, Santa Clara, CA) using SensiMix SYBR kits (Bioline, Tauton, MA). Amplification was performed at 95°C for 10 min, followed by 40 cycles of 95°C for 15 sec, and 60°C for 1min. For mature miRNA expression: the universal primer provided in the NCodeTM miRNA first-strand cDNA synthesis kit was used together with one of the following forward primers:

Mmu-miR-21 (MIMAT0000530): 5′ TAGCTTATCAGACTGATGTTGA 3′

Mmu-miR-210 (MIMAT0000658): 5′ CTGTGCGTGTGACAGCGGCTGA 3′

U6 snRNA: 5′ ACACGCAAATTCGTGAAGC 3′

Exosome labeling with PKH26

Purified exosomes/microvesicles were labeled with PKH26 red fluorescent labeling kits (Sigma-Aldrich, St. Louis, MO) according to the manufacturer's instructions. The labeled exosomes/microvesicles were stained with PKH26 dye in 400ul Diluent C fluid for 5 minutes at room temperature. An equal volume of exosome-depleted serum was added to terminate the labeling reaction, and exosomes/microvesicles were re-purified via PEG precipitation. H9C2, a rat cardiomyoblast cell line, was obtained from American Type Culture Collection (Rockville, MD), and cells were cultured in DMEM medium supplemented with 10% exosome-depleted FBS, 100 U/mL penicillin, and 100 μg/mL streptomycin. The H9C2 cells were incubated with 5μl labeled iPS-exo for 0, 2hrs, 10hrs, or

14hrs in a 12 well plate at 37°C and then washed with phosphate-buffered saline (PBS). Nuclear staining was performed using NuBlue® Live Cell Stain ReadyProbes™ reagent (Life Technologies, Carlsbad, CA). Uptake of labeled exosomes/microvesicles by H9C2 cells was determined using an inverted fluorescence microscope.

Caspase 3/7 activity assay

For oxidative stress-induced apoptosis assay, H9C2 cells were incubated in DMEM medium with 2% exosome-depleted FBS medium supplemented with 2μl CF-exo, iPS-exo, or vehicle (PBS) for 14 hrs (10,000 cells/well in 96-well plate), and then not subjected or subjected to oxidative stress (200 μM H_2O_2 for 4 h). Following treatment, activity of Caspase-3 and -7 in H9C2 cells was assayed with Caspase-Glo 3/7 Assay System (Promega, Madison) according to the manufacturer's instructions.

Murine myocardial ischemia model and intramyocardial iPS or exosome delivery

To assess the pluripotency of iPS cells generated from mouse CF, Male C57/BL6 mice were anesthetized with ketamine/xylazine (100 mg/kg/10mg/kg, i.p.) and mechanically ventilated. Myocardial infarction was induced via ligation of the left anterior descending coronary artery 2 mm from the tip of the normally positioned left atrium as we described previously[7, 11]. A 30 μl solution containing 5×10^5 iPS cells in DMEM was injected intramyocardially 1mm above the ligation site immediately after induction of MI. To assess the effect of iPS-exo on protecting cardiomyocytes from acute myocardial ischemia/reperfusion (MIR) induced apoptosis in vivo, mice were subjected to acute MIR as described previously[9]. Briefly, 2–3 month old, male C57BL/6 mice were anesthetized with intraperitoneal injection of 100mg/kg ketamine combined with 10mg/kg xylazine. Mice were intubated transorally with a 24-gauge tube and ventilated with room air using a Harvard rodent ventilator (Inspira Advenced Safety Ventilator Model 55–7058, Holliston, MA). The chest was opened via a lateral thoracotomy, and the heart was exposed through pericardiotomy. An 8-0 nylon suture (Ethicon, Somerville, NJ) was placed under the left coronary artery and then threaded through a small plastic (PE10) tube to form a snare for reversible occlusion. Intramyocardial injections of PBS, CF-exo and iPS-exo (25μl) were performed on mice immediately after induction of ischemia by coronary occlusion in one site in ischemic zone (Supple. Fig.2; n = 9 per group, 3 hearts for Western blots, and 6 hearts for histological assays). The left coronary artery was occluded for 45 minutes, and then reperfusion was established by gently removing the tube. The chest was closed and the mice were allowed to recover. Animals were sacrificed at 24 hours after reperfusion for tissue harvesting and histological assays. Animals were handled according to approved protocols and animal welfare regulations of the Institutional Animal Care and Use Committee of the Medical College of Georgia.

Histology

For cell staining, iPS were plated on 8-well chamber slides (Millipore, Billerica, MA) and fixed with 4% paraformaldehyde. After blocked with avidin/biotin blocking solution (Thermo scientific) followed by Mouse-on-Mouse kit (Vector Laboratories) according to the manufacturer's instruction, cells were incubated with mouse anti-stage-specific embryonic antigen-1 (SSEA1) antibody (1:50; Chemicon, Temecula, CA) or rabbit anti-Nanog (1:1000;

Cell Signaling) at 4°C overnight. Primary antibodies were resolved via secondary staining with Streptavidin Alexa Fluor 555 conjugate (1:400, Life Technologies, Carlsbad, CA) or goat anti-rabbit Alexa Fluor 555 conjugated (1:400, Life Technologies, Carlsbad, CA). Slides were mounted using VECTASHIELD HardSet Mounting Medium with DAPI (Vector Laboratories, Burlingame, CA).

For tissue staining to assess the pluripotency of iPS cells generated from mouse CF, two weeks post cell therapy, mouse hearts were harvested, embedded in OCT compound, snap-frozen, cut into 5-μm sections, and immunostained with anti-α-Fetoprotein (AFP) (1:50; Thermo Pierce, Rockford, IL), anti-chromogranin A (1:50; Thermo Pierce, Rockford, IL) and anti-tyrosine hydroxylase (TH) (1:50; Cell signaling, Danvers, MA) antibodies. Primary antibodies were resolved via secondary staining with goat anti-rabbit Alexa Fluor 555 conjugated (1:400, Life Technologies, Carlsbad, CA). Nuclei were counterstained with DAPI (Vector Laboratories, Burlingame, CA).

To quantify apoptotic cardiomyocytes in mouse model of myocardial ischemia/reperfusion injury, mouse hearts were removed 24 h after reperfusion, fixed with 30% sucrose, frozen embedded in OCT and processed for sectioning and staining with terminal deoxynucleotidyl transferase dUTP nick end labeling (TUNEL) and cardiac Troponin I (cTnI) (1:50, Santa Cruz Biotechnology, Santa Cruz, CA). TUNEL was performed using The DeadEnd™ Fluorometric TUNEL System (Promega) per the manufacturer's protocol with minor modifications. The slides were incubated with Alexa 488-conjugated anti-rabbit secondary antibodies and Streptavidin Alexa Fluor 555 conjugate (1:400, Life Technologies, Carlsbad, CA). (Invitrogen). Slides were mounted using VECTASHIELD HardSet Mounting Medium with DAPI (Vector Laboratories). The staining was analyzed by a Zeiss 710 Laser Scanning Microscope (Carl Zeiss, Thornwood, NY). Apoptotic cardiomyocytes were quantified and classified as TUNEL(+) cTnI(+).

Statistical Analysis

Results are presented as the mean ± standard error of the mean (SEM). Comparisons between groups were made by one-way analysis of variance or two-tailed Student's t test. Differences were considered statistically significant at $p < 0.05$

Results

Characterization of CF derived iPS

We derived cardiac fibroblast cells (CF) from C57BL/6 mouse hearts. CF are frequently contaminated with cardiac stem cells (CSC), which express c-kit and/or sca-1 cell surface markers. To obtain a pure population of CF, we used negative MACS to remove c-kit+ and sca-1+ cell populations from CF. Cultured CF were flat, spindle-shaped cells (Fig. 1A) staining negative for alkaline phosphatase (Fig. 1C). To generate iPS cells, we use lentiviral vectors to ectopically express OCT4, SOX2, KLF4 and c-MYC in CF. Colonies with mouse ES cell-like, dome-shaped morphology were selected and expanded. The CF-iPS colonies exhibited defined borders (Fig. 1B) and alkaline phosphatase positivity (Fig.1D). SSEA1 and Nanog are markers for mouse ES cell identification and selection[12]. Thus, we

evaluated the CF-iPS colonies and found that they all stained positively for SSEA1 and Nanog (Fig. 1E–F). To investigate the pluripotency of transplanted CF-derived iPS cells in ischemic myocardium, iPS cells were injected into the mouse ischemic myocardium. After 2 weeks, we observed that the iPS cells differentiated into liver cells (Fig. 1G), neuroendocrine cells (Fig. 1H) and adrenergic neuron cells (Fig. 1I), suggesting the pluripotency of CF-iPS. The cardiomyocyte differentiation of iPS cells was reported by us previously [24].

Characterization of iPS-exosomes/microvesicles

Exosomes/microvesicles were readily detectable in media from CF and iPS after PEG precipitation. Morphological analysis of the CF-exosomes/microvesicles and iPS-exosomes/microvesicles using electron micrography demonstrated grape-like clusters of nanoparticle exosomes/microvesicles (Fig. 2A–B). We quantified exosomes/microvesicles using standard Bradford assay, a standard protein quantification method. Western blot analysis of CF-exosomes/microvesicles and iPS-exosomes/microvesicles revealed the presence of exosome markers CD63 and Tsg101 (Fig. 2C). The size of pelleted structures was determined with dynamic light scattering (DLS) using a ZetaView®, a nanoparticle tracking analyzer for hydrodynamic particle size. The pellets consisted of particles with an average size of 100 nm in diameter, consistent with characteristic size range of exosomes/microvesicles (Fig. 2D–E). For the zeta potential, after optimization, we have specifically selected 0.05X PBS (diluted 20X from 1X PBS) as the buffer. The conductivity of 0.05X PBS is around 500 uS/cm. The zeta potentials for CF and IPS exosomes are very similar −14.22mV vs. −15.44 mV at 23°C. The measured zeta potential indicates that these exosomes are not very stable in the solution at 23°C (Fig. 2F–G). Temperature affects zeta potential positively, the zeta potential for CF-exo and iPS-exo are very similar with −23.85 mv vs. −23.93 mv at 37°C (Supple. Fig. 3).

Exosome labeling and uptake by H9C2

To determine whether iPS-exo can be efficiently taken up by cardiomyocytes in vitro, we labeled iPS-exosomes/microvesicles with PKH26, a fluorescent cell linker compound that is incorporated into the cell membrane by selective partitioning. The labeled exosomes/microvesicles were then incubated with H9C2 cells, which were examined for fluorescence at varying time points. Within two hrs after PKH26-labeled exosomes/microvesicles were added to the culture medium, red fluorescence signals were detected in the H9C2 cells (Fig. 3A). By 14 hrs, nearly every H9C2 cell exhibited red fluorescence. These finding suggest that iPS-exo are readily taken up by H9C2 cells and thus potentially could be used therapeutically to modulate cardiomyocyte function.

Anti-apoptotic effects of iPS-exo on H9C2 cells under oxidative stress

In order to determine the effects of exosomes/microvesicles on cardiomyocyte apoptosis induced by oxidative stress, the H9C2 cells were pretreated with PBS, CF-exo or iPS-exo and then subjected to acute H_2O_2 oxidative stress or not. We measured caspase-3/7 activation among the three groups of cells. As shown in Fig. 3B, caspase activation was decreased in H9C2 cells treated with either CF-exo or iPS-exo, but iPS-exo were

substantially more effective than CF-exo at protection against H_2O_2-induced caspase activation.

In vivo anti-apoptotic effects of iPS-exo in the MIR model

To determine whether iPS-exo treatment affects heart function in vivo, we assess cardiac function in mice before, and one day after iPS-exo treatment. Cardiac function analyses by echocardiographic measurements indicated that there is no significant change in both left-ventricular ejection fraction and fractional shortening in mice administered iPS-exo (Supple. Fig. 1).

We next determined whether iPS-exo administration in vivo would afford protection against acute ischemia/reperfusion-induced cardiomyocyte apoptosis. We injected PBS, CF-exo or iPS-exo intramyocardially immediately after induction of ischemia by left coronary occlusion and assayed TUNEL (+)/cTnI (+) apoptotic cardiomyocytes 24 hrs post reperfusion. Delivery of either CF-exo or iPS-exo to ischemic myocardium before reperfusion significantly reduced cardiomyocyte apoptosis compared with PBS control (Fig. 4 A–D). However, iPS-exo treatment was considerably more effective than CF-exo ($P<0.05$, $n=6$), suggesting iPS-exo exhibit enhanced cytoprotective effects in the setting of MIR.

iPS-exo suppress pro-apoptotic proteins in ischemic myocardium

To identify the mechanisms of iPS-exo mediated cytoprotection, we measured the level of active caspase 3, the key effector of apoptosis in the apoptotic pathway [13], in ischemic hearts treated with PBS, CF-exo or iPS-exo. Our data, presented in Fig 5A–B, show that iPS-exo treatment reduced active caspase3 proteins in ischemic myocardium in comparison with CF-exo treatment and PBS control treatment. These findings suggest that iPS-exo pre-treatment more effectively suppresses apoptosis in the ischemic myocardium, thereby leading to enhance cytoprotective effects.

Exosomes/microvesicles mediate the transfer of cardioprotective miRNAs from iPS cells to H9C2 cells

miR-21 and miR -210 are two major cardioprotective miRNAs which are regulated by Nanog[14] and hypoxia-inducible factor-1 α (HIF-1α)[15], respectively, and have been reported to protect cardiomyocytes against apoptosis[16, 17]. CF-iPS express higher protein levels of Nanog and HIF-1α than CF (Fig. 6A1–2). We quantified relative levels of miR-21 and miR-210 in exosomes/microvesicles by real time RT-PCR and found that miR-21 and miR-210 levels were markedly increased in iPS-exo compared with CF-exo (Fig. 6B–C), suggesting the enrichment of cardioprotective microRNAs in iPS-exo. Recent studies suggest that exosomes/microvesicles can transfer lipid-associated miRNAs between cells by various routes, including endocytotic uptake, membrane-fusion, and scavenger receptors[18]. To determine if iPS-exo carrying miR-21 and miR-210 can deliver the miRNA into cardiomyocytes, we exposed H9C2 cells to iPS-exo or CF-exo for 14 h. The levels of miR-21 and miR-210 in iPS-exo-treated H9C2 cells were approximately 3-fold and 5-fold higher, respectively compared to CF-exo-treated cells (Fig. 6D–E). Thus, iPS-exo can deliver cardioprotective miRNAs into cardiomyocytes in vitro, suggesting a novel mechanism for iPS-exo-mediated cardioprotection.

Discussion

Cell-based therapy using iPS cells is a potentially promising means to improve cardiac function in the ischemic milieu. However, the use of iPS cells may be compromised by their tumorigenic potential. Here, we demonstrate that exosomes/microvesicles secreted from iPS cells can be taken up into cardiomyoyctes efficiently in vitro, thus producing significant cytoprotection against oxidative stress. Transplantation of iPS-exo into ischemic myocardium significantly suppressed active caspase3 protein expression and protected against cardiomyocyte apoptosis in vivo. Mechanistically, cardioprotective miR-21 and miR-210, regulated by Nanog and HIF-1α respectively, are highly enriched in iPS-exo and efficiently transmitted to cardiomyocytes through exosomal-cell communications.

Adult somatic cells can be reprogrammed to induced pluripotent stem (iPS) cells by the four stem specific transcription factors, Oct4, Sox2, Klf4, and c-Myc[19]. IPS cells can differentiate into cardiovascular cell lineages for heart repair [19–22]. Protocols for iPS cardiomyocyte differentiation have been continuously refined, leading to enhanced efficiency [23]. However, tumorigenicity in vivo remains a crucial challenge to the therapeutic application of iPS cells [24, 25]. Indeed, in contrast to most engrafted adult stem cells, including cardiac stem cells and bone marrow-derived mesenchymal stem cells, which quickly die within ischemic myocardium, transplanted iPS cells can survive and form tumors in ischemic myocardium [26]. The mechanisms underlying the enhanced survivability of iPS cells in ischemic myocardium are unclear. Stem cell derived exosomes/microvesicles have been reported to elicit pro-survival and pro-angiogenic effects in ischemic myocardium[9, 27]. We demonstrated that exosomes/microvesicles can protect H9C2 cells from apoptosis induced by oxidative stress. Moreover, iPS-exo protect ischemic cardiomyocytes from apoptosis induced by acute MIR in vivo. Our data raise the possibility that exosomes/microvesicles secreted by iPS cells may be able to transmit survival signals from iPS cells to neighboring cardiomyocytes.

IPS-derived exosomes might not be dangerous for transdifferentiation of cardiomyocytes. Compared to other tissue cells, cardiomyocytes are much difficult to be transdifferentiated by iPS genes, Abad M. et al. [28] recent work demonstrated the order of incidence of transdifferentiation in different tissue cells as below: pancreas>kidney>Intestine>Adipose tissue>Liver>Intracranial>Stomach. Zeta potential is a physical property of exosomes by measuring the magnitude of electrostatic or charge repulsion or attraction between particles, it affect stability of exosomes[29]. Nanoparticles is stable at the absolute values of the zeta potential in the range from 31 to 40mV[30]. In our measurement, both iPS-exo and CF-exo have a zeta potential of −14mV to −15mV at 23°C, which is consistent with other report, which shows exosomes had a zeta potential of −14.54±1.31mV[31]. Therefore, exosomes is instable, and have a tendency for aggregation (Fig. 2A–B), sonication was commonly used to disperse aggregated exosomes [32, 33]. Temperature affects zeta potential, which increased about 0.39% per °C[34], indicating exosomes might increase stability in tissues in vivo. Our result shows that the zeta potential for CF-exo and IPS-exo are very similar with −23.85 mv vs. −23.93 mv at 37 °C (Supple. Fig. 3).

MiRNA are evolutionarily conserved, small, non-coding RNA molecules that modulate cell differentiation, proliferation, and apoptosis via post-transcriptional repression[35]. The mechanisms of iPS-exo-mediated cytoprotection may be related to their miRNA contents, which are remarkably stable[36]. We demonstrated that the iPS- exo contained high levels of pro-survival microRNAs, including miR-21 and miR-210, in comparison with CF-exosomes/microvesicles. The higher levels of expression of these miRNAs may be directly related to Nanog, an embryonic stem cell-specific transcription factor, and the key hypoxia related transcription factor HIF-1α. Bourguignon et al[14] reported that Nanog signaling promotes miR-21 expression, while Nanog-specific small interfering RNA (siRNA) treatment can abrogate miR-21 production, suggesting that miR-21 is an important downstream component of Nanog signaling. Hypoxia is a characteristic of the embryonic stem cell niche and plays a critical role in early embryonic development. HIF-1α signaling is active in pluripotent stem cells[37], and miR-210 is a direct HIF-1α-regulated microRNA[16] that plays an important role in cardioprotection[38]. Mutharasan et al [38] reported that overexpression of miR-210 reduced reactive oxygen species (ROS) production and cell death in response to oxidative stress, while downregulation of miR-210 increased ROS after hypoxia-reoxygenation. Kim et al [16] reported that the cytoprotective effect of miR-210 is mediated by FLICE-associated huge protein (FLASH)/caspase-8-associated protein-2 (Casp8ap2) suppression. Our findings that iPS-exo dramatically reduce activate Caspase3 expression in ischemic myocardium in vivo could in part be due to transmission of specific miRNAs such as miR-210.

Limitations

Compared to cell therapy, exosomes are much safe for bench-to bedside translation, however, there are also many limitations (1) exosomes cannot differentiate into tissue cells; (2) exosomes might have only short term beneficial effect due to their short half-life, but engrafted donor stem cell can continuously release exosome, and have long term beneficial effect; (3) exosomes have pro-fibroblast effect, a recent study reported that iPS derived exo can facilitate cutaneous wound healing by promoting collagen synthesis and angiogenesis[39]. Fibroblasts are important to prevent cardiac rupture after acute myocardial infarction [40], therefore, in the short term, iPS-exo treatment might reduce the risk of acute heart rupture, however, in the long term, increased proliferation of fibroblast can increase scarring, leading to left ventricular remodeling; (4). In this study, we only test the anti-apoptosis capacity of iPS-exo in ischemic cardiomyocytes by using acute myocardial ischemia/reperfusion model, this model cannot address whether iPS-exo might influence the proliferation of other cells, including fibroblasts and cardiac progenitor cells, in ischemic myocardium (Fig. 7). Since exosome study is still at early stage, we need more future study on what grossly happened in myocardium.

Conclusions

Exosomes/microvesicles secreted by iPS can convey survival signals to ischemic myocardium that protect cardiomyocytes against acute myocardial ischemia/reperfusion injury in vivo, The mechanisms may be related to miRNA-mediated cytoprotection leading to inhibition of myocardial apoptosis. These findings highlight for the first time the therapeutic potential of iPS-derived exosomes/microvesicles in cardioprotection.

Supplementary Material

Refer to Web version on PubMed Central for supplementary material.

Acknowledgments

This work was supported by the American Heart Association Beginning Grant-in-Aid 0765094Y (to Y.T.); NIH grant HL086555 (to Y.T.), and NIH grants HL076684 and HL62984 (to N.L.W.), National Natural Science Foundation of China (No. 81270203, to L.C.). Science and technology commission of Shanghai municipality 12ZR1432600 (to X.L.W.).

References

1. Buja LM, Vela D. Cardiomyocyte death and renewal in the normal and diseased heart. Cardiovascular pathology : the official journal of the Society for Cardiovascular Pathology. 2008; 17:349–74. [PubMed: 18402842]
2. Tang YL, Wang YJ, Chen LJ, Pan YH, Zhang L, Weintraub NL. Cardiac-derived stem cell-based therapy for heart failure: progress and clinical applications. Experimental biology and medicine. 2013; 238:294–300. [PubMed: 23598975]
3. Forristal CE, Christensen DR, Chinnery FE, Petruzzelli R, Parry KL, Sanchez-Elsner T, et al. Environmental oxygen tension regulates the energy metabolism and self-renewal of human embryonic stem cells. PloS one. 2013; 8:e62507. [PubMed: 23671606]
4. Cai H, Lin L, Cai H, Tang M, Wang Z. Prognostic evaluation of microRNA-210 expression in pediatric osteosarcoma. Medical oncology. 2013; 30:499. [PubMed: 23430441]
5. Lee PY, Chien Y, Chiou GY, Lin CH, Chiou CH, Tarng DC. Induced pluripotent stem cells without c-Myc attenuate acute kidney injury via downregulating the signaling of oxidative stress and inflammation in ischemia-reperfusion rats. Cell transplantation. 2012; 21:2569–85. [PubMed: 22507855]
6. Stoorvogel W. Functional transfer of microRNA by exosomes. Blood. 2012; 119:646–8. [PubMed: 22262739]
7. Zhang L, Pan Y, Qin G, Chen L, Chatterjee TK, Weintraub NL, et al. Inhibition of stearoyl-coA desaturase selectively eliminates tumorigenic Nanog-positive cells: Improving the safety of iPS cell transplantation to myocardium. Cell Cycle. 2014:13. [PubMed: 24270859]
8. Lee C, Mitsialis SA, Aslam M, Vitali SH, Vergadi E, Konstantinou G, et al. Exosomes mediate the cytoprotective action of mesenchymal stromal cells on hypoxia-induced pulmonary hypertension. Circulation. 2012; 126:2601–11. [PubMed: 23114789]
9. Chen L, Wang Y, Pan Y, Zhang L, Shen C, Qin G, et al. Cardiac progenitor-derived exosomes protect ischemic myocardium from acute ischemia/reperfusion injury. Biochemical and biophysical research communications. 2013; 431:566–71. [PubMed: 23318173]
10. Hu G, Yao H, Chaudhuri AD, Duan M, Yelamanchili SV, Wen H, et al. Exosome-mediated shuttling of microRNA-29 regulates HIV Tat and morphine-mediated neuronal dysfunction. Cell Death Dis. 2012; 3:e381. [PubMed: 22932723]
11. Chen L, Wang Y, Pan Y, Zhang L, Shen C, Qin G, et al. Cardiac progenitor-derived Exosomes protect ischemic myocardium from acute ischemia/reperfusion injury. Biochemical and biophysical research communications. 2013
12. Brambrink T, Foreman R, Welstead GG, Lengner CJ, Wernig M, Suh H, et al. Sequential expression of pluripotency markers during direct reprogramming of mouse somatic cells. Cell stem cell. 2008; 2:151–9. [PubMed: 18371436]
13. Nicholson DW, Ali A, Thornberry NA, Vaillancourt JP, Ding CK, Gallant M, et al. Identification and inhibition of the ICE/CED-3 protease necessary for mammalian apoptosis. Nature. 1995; 376:37–43. [PubMed: 7596430]
14. Bourguignon LY, Earle C, Wong G, Spevak CC, Krueger K. Stem cell marker (Nanog) and Stat-3 signaling promote MicroRNA-21 expression and chemoresistance in hyaluronan/CD44-activated head and neck squamous cell carcinoma cells. Oncogene. 2012; 31:149–60. [PubMed: 21685938]

15. Pulkkinen K, Malm T, Turunen M, Koistinaho J, Yla-Herttuala S. Hypoxia induces microRNA miR-210 in vitro and in vivo ephrin-A3 and neuronal pentraxin 1 are potentially regulated by miR-210. FEBS letters. 2008; 582:2397–401. [PubMed: 18539147]
16. Kim HW, Haider HK, Jiang S, Ashraf M. Ischemic preconditioning augments survival of stem cells via miR-210 expression by targeting caspase-8-associated protein 2. The Journal of biological chemistry. 2009; 284:33161–8. [PubMed: 19721136]
17. Sayed D, He M, Hong C, Gao S, Rane S, Yang Z, et al. MicroRNA-21 is a downstream effector of AKT that mediates its antiapoptotic effects via suppression of Fas ligand. The Journal of biological chemistry. 2010; 285:20281–90. [PubMed: 20404348]
18. Vickers KC, Remaley AT. Lipid-based carriers of microRNAs and intercellular communication. Current opinion in lipidology. 2012; 23:91–7. [PubMed: 22418571]
19. Takahashi K, Yamanaka S. Induction of pluripotent stem cells from mouse embryonic and adult fibroblast cultures by defined factors. Cell. 2006; 126:663–76. [PubMed: 16904174]
20. Takahashi K, Tanabe K, Ohnuki M, Narita M, Ichisaka T, Tomoda K, et al. Induction of pluripotent stem cells from adult human fibroblasts by defined factors. Cell. 2007; 131:861–72. [PubMed: 18035408]
21. Narazaki G, Uosaki H, Teranishi M, Okita K, Kim B, Matsuoka S, et al. Directed and systematic differentiation of cardiovascular cells from mouse induced pluripotent stem cells. Circulation. 2008; 118:498–506. [PubMed: 18625891]
22. Ohnuki M, Takahashi K, Yamanaka S. Generation and characterization of human induced pluripotent stem cells. Current protocols in stem cell biology. 2009; Chapter 4(Unit 4A):2. [PubMed: 19536759]
23. Ye L, Zhang S, Greder L, Dutton J, Keirstead SA, Lepley M, et al. Effective cardiac myocyte differentiation of human induced pluripotent stem cells requires VEGF. PloS one. 2013; 8:e53764. [PubMed: 23326500]
24. Lee AS, Tang C, Rao MS, Weissman IL, Wu JC. Tumorigenicity as a clinical hurdle for pluripotent stem cell therapies. Nature medicine. 2013; 19:998–1004.
25. Liu Z, Tang Y, Lu S, Zhou J, Du Z, Duan C, et al. The tumourigenicity of iPS cells and their differentiated derivates. Journal of cellular and molecular medicine. 2013; 17:782–91. [PubMed: 23711115]
26. Tang YL, Zhu W, Cheng M, Chen L, Zhang J, Sun T, et al. Hypoxic preconditioning enhances the benefit of cardiac progenitor cell therapy for treatment of myocardial infarction by inducing CXCR4 expression. Circulation research. 2009; 104:1209–16. [PubMed: 19407239]
27. Lai RC, Yeo RW, Tan KH, Lim SK. Mesenchymal stem cell exosome ameliorates reperfusion injury through proteomic complementation. Regenerative medicine. 2013; 8:197–209. [PubMed: 23477399]
28. Abad M, Mosteiro L, Pantoja C, Canamero M, Rayon T, Ors I, et al. Reprogramming in vivo produces teratomas and iPS cells with totipotency features. Nature. 2013; 502:340–5. [PubMed: 24025773]
29. Marimpietri D, Petretto A, Raffaghello L, Pezzolo A, Gagliani C, Tacchetti C, et al. Proteome profiling of neuroblastoma-derived exosomes reveal the expression of proteins potentially involved in tumor progression. PloS one. 2013; 8:e75054. [PubMed: 24069378]
30. Ostolska I, Wisniewska M. Application of the zeta potential measurements to explanation of colloidal CrO stability mechanism in the presence of the ionic polyamino acids. Colloid Polym Sci. 2014; 292:2453–64. [PubMed: 25242857]
31. Jo W, Jeong D, Kim J, Cho S, Jang SC, Han C, et al. Microfluidic fabrication of cell-derived nanovesicles as endogenous RNA carriers. Lab on a chip. 2014; 14:1261–9. [PubMed: 24493004]
32. Ansa-Addo EA, Lange S, Stratton D, Antwi-Baffour S, Cestari I, Ramirez MI, et al. Human plasma membrane-derived vesicles halt proliferation and induce differentiation of THP-1 acute monocytic leukemia cells. J Immunol. 2010; 185:5236–46. [PubMed: 20921526]
33. Maas SL, De Vrij J, Broekman ML. Quantification and size-profiling of extracellular vesicles using tunable resistive pulse sensing. Journal of visualized experiments : JoVE. 2014:e51623. [PubMed: 25350417]

34. Evenhuis CJ, Guijt RM, Macka M, Marriott PJ, Haddad PR. Variation of zeta-potential with temperature in fused-silica capillaries used for capillary electrophoresis. Electrophoresis. 2006; 27:672–6. [PubMed: 16400701]

35. Carleton M, Cleary MA, Linsley PS. MicroRNAs and cell cycle regulation. Cell Cycle. 2007; 6:2127–32. [PubMed: 17786041]

36. Creemers EE, Tijsen AJ, Pinto YM. Circulating microRNAs: novel biomarkers and extracellular communicators in cardiovascular disease? Circulation research. 2012; 110:483–95. [PubMed: 22302755]

37. Silvan U, Diez-Torre A, Arluzea J, Andrade R, Silio M, Arechaga J. Hypoxia and pluripotency in embryonic and embryonal carcinoma stem cell biology. Differentiation; research in biological diversity. 2009; 78:159–68.

38. Mutharasan RK, Nagpal V, Ichikawa Y, Ardehali H. microRNA-210 is upregulated in hypoxic cardiomyocytes through Akt- and p53-dependent pathways and exerts cytoprotective effects. American journal of physiology Heart and circulatory physiology. 2011; 301:H1519–30. [PubMed: 21841015]

39. Zhang J, Guan J, Niu X, Hu G, Guo S, Li Q, et al. Exosomes released from human induced pluripotent stem cells-derived MSCs facilitate cutaneous wound healing by promoting collagen synthesis and angiogenesis. Journal of translational medicine. 2015; 13:49. [PubMed: 25638205]

40. Matsui Y, Ikesue M, Danzaki K, Morimoto J, Sato M, Tanaka S, et al. Syndecan-4 prevents cardiac rupture and dysfunction after myocardial infarction. Circulation research. 2011; 108:1328–39. [PubMed: 21493899]

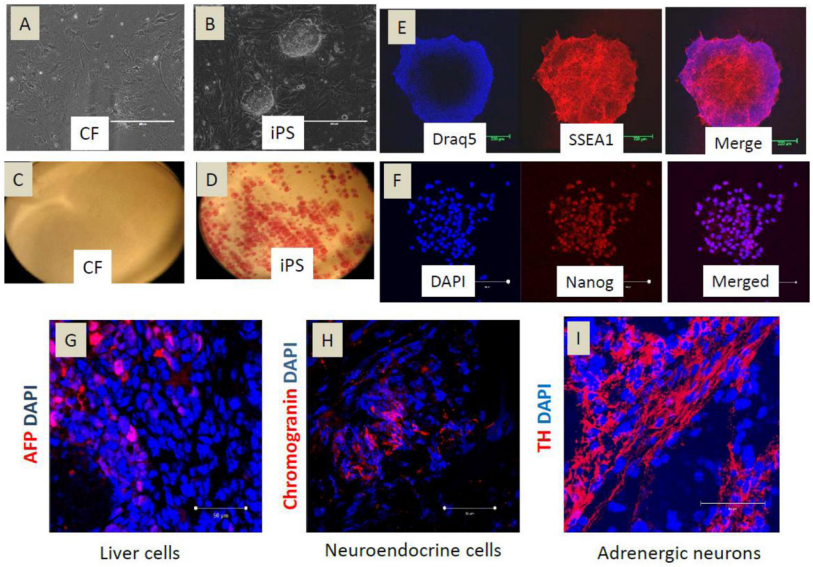

Figure 1.

Characterization of CF-derived induced pluripotent stem cells. (**A–B**) Mouse CF and CF-derived iPS cultured on dishes; (**C–D**) alkaline phosphatase staining of cultured cells; (**E**) Immunofluorescent staining of iPS cells for the classic ES cell marker SSEA-1 (red). Nuclei were stained with Draq5 (blue); (**F**) Immunofluorescent staining of iPS cells for the classic ES cell marker Nanog (red). Nuclei were stained with DAPI (blue); (**G–I**) Immunofluorescent staining for AFP (liver cells), Chromogranin A (neuroendocrine cells), and Tyrosine hydrolase (TH) (adrenergic neuron cells) of heart sections 2 weeks after cell transplantation in heart.

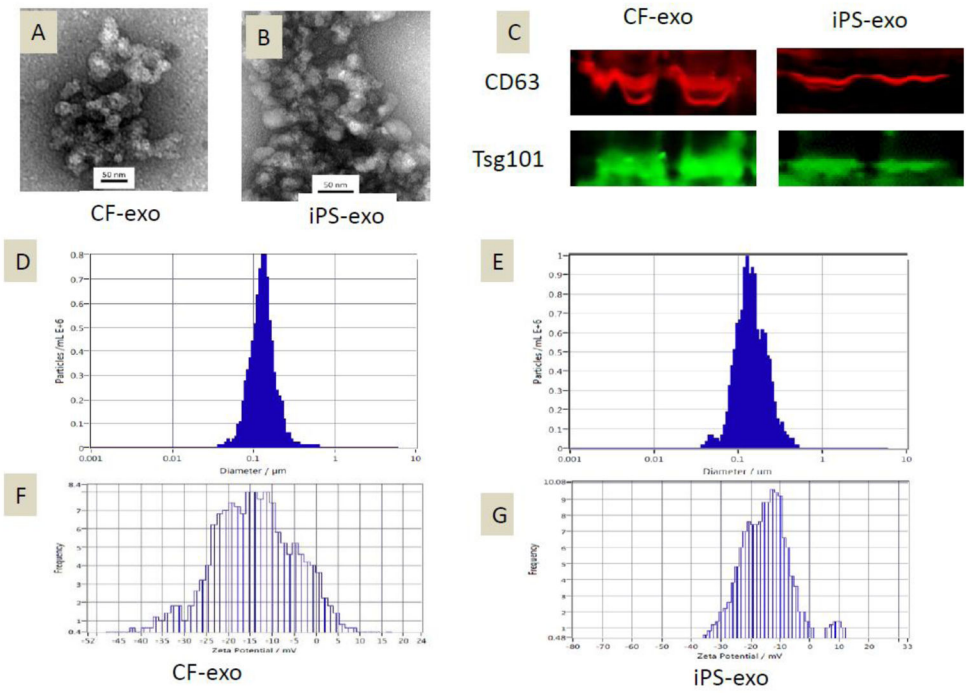

Figure 2.

Characterization of CF-exosomes/microvesicles and iPS-exosomes/microvesicles. (**A–B**) Electron micrograph image of CF-derived and iPS-derived exosomes/microvesicles. The image shows a mass of round-shaped vesicles that resemble a cluster of grapes. Scale bar=50nm. **(C)** Western blot results demonstrate the expression of CD63 and Tsg101 in exosomes/microvesicles derived from CF and iPS. (**D–E**) Particle size distribution in purified pellets consistent with size range of exosomes/microvesicles (average size 100 nm), measured by ZetaView® Particle Tracking Analyzer. (**F–G**) Zeta potential of CF-exo and iPS-exo at 23°C.

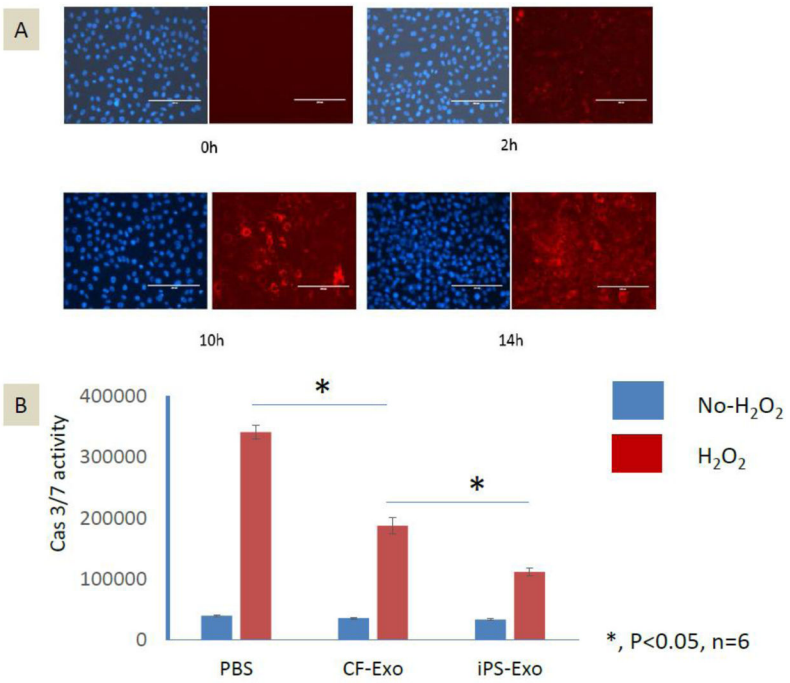

Figure 3.

Time course of cellular uptake of exosomes/microvesicles and effects on H_2O_2-induced caspase activation in H9C2 cells. **(A)** Time course (0–14 hrs) of uptake of PKH26-labeled-exosomes/microvesicles by H9C2 cells in vitro. Red dots indicate exosomes/microvesicles incorporated into H9C2 cells. (**B**) Caspase-3/7 activity assay in H9C2 cells treated with PBS control, CF-exo or iPS-exo and subjected or not subjected to oxidative stress (200μM H_2O_2 for 4hs). *, P<0.05, n=6.

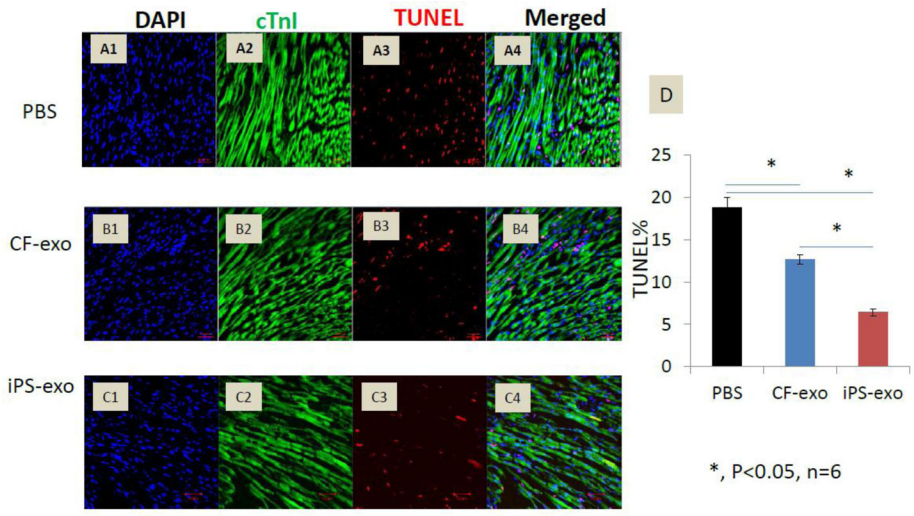

Figure 4.

Transplantation of iPS-exo significantly reduced cardiomyocyte apoptosis in ischemic myocardium. (**A–C**) Heart sections from PBS, CF-exo, or iPS-exo treated mice were co-stained with TUNEL and cTnI antibody. Representative images of TUNEL staining in heart sections after 45min ischemia and 24h reperfusion are shown. Red staining indicates TUNEL-positive cells, and green staining indicates cTnI positive cardiomyocytes. (**D**) Quantification of apoptotic cardiomyocytes, *, $P < 0.05$, n=6.

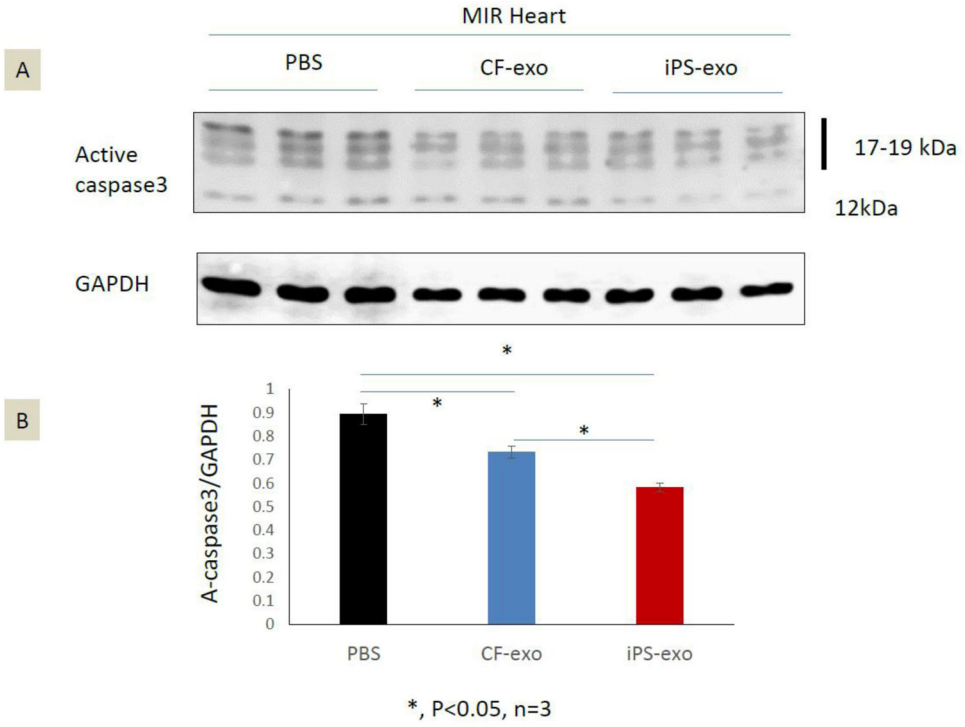

Figure 5.

iPS-exo treatment reduced the active Caspase 3 protein in ischemic myocardium. (**A–B**) The level of active caspase 3 protein in ischemic hearts treated with PBS, CF-exo or iPS-exo. Total heart proteins were analyzed by SDS-PAGE and immunoblotted for active caspase3; GAPDH served as a loading control. *, P<0.05, n=3.

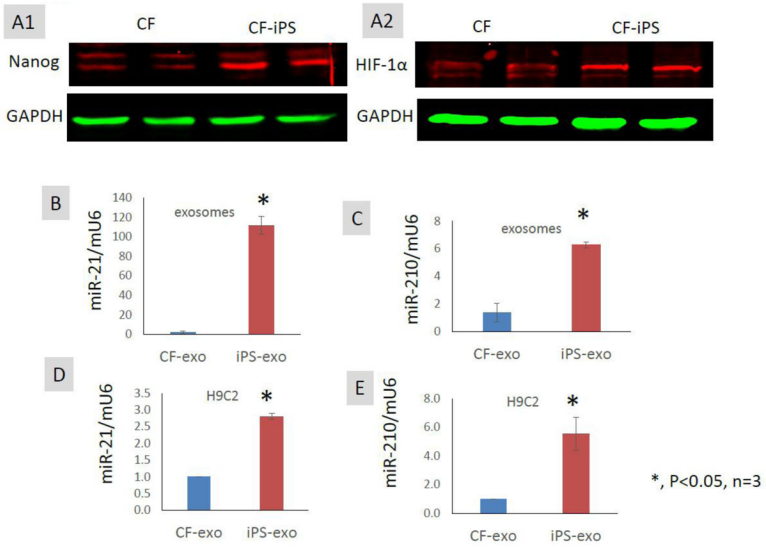

Figure 6.

Exosomes/microvesicles mediate the transfer of cardioprotective miR-21 and miR-210 to H9C2 cells in vitro. **(A1–2)** Comparison of Nanog and HIF-1α in CF versus iPS by Western blot. **(B–C)** Comparison of cardioprotective miR-21 and miR-210 expression in iPS-exo versus CF-exo. Real-time RT-PCR shows the expression of miR-21 and miR-210 was significantly higher in iPS-exo compared with CF-exo. Mouse U6 snRNA was used as a normalization reference in real-time PCR. **(C–D)** miR-21 and miR-210 expression (RT-PCR) in H9C2 cells after treatment with CF-exo or iPS-exo (n = 3).

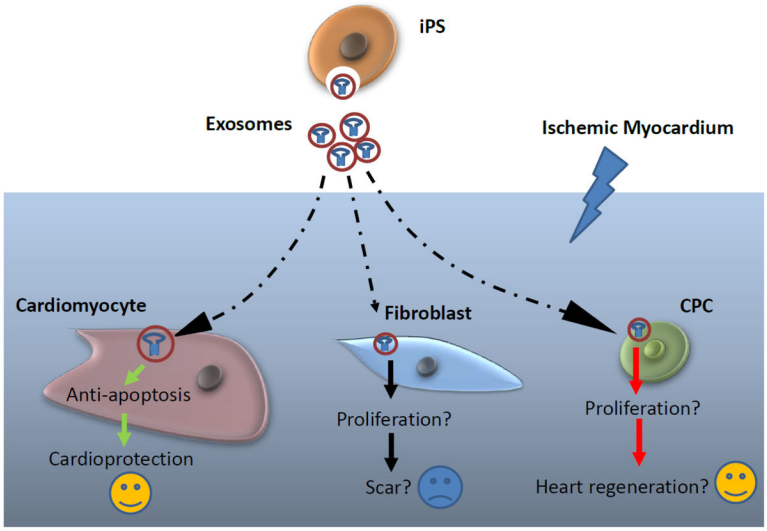

Figure 7.

Schematic representation of the impact of iPS-exo on cardiomyocytes, fibroblasts and cardiac progenitor cells in hearts post-ischemia/reperfusion injury.